JACS
JOURNAL OF THE AMERICAN CHEMICAL SOCIETY
Article
pubs.acs.org/JACS

Quantitation of Femtomolar Protein Levels via Direct Readout with the Electrochemical Proximity Assay

Jiaming Hu,† Tanyu Wang,† Joonyul Kim, Curtis Shannon,* and Christopher J. Easley*

Department of Chemistry and Biochemistry, Auburn University, Auburn, Alabama 36849, United States

ABSTRACT: We have developed a separation-free, electrochemical assay format with direct readout that is amenable to highly sensitive and selective quantitation of a wide variety of target proteins. Our first generation of the electrochemical proximity assay (ECPA) is composed of two thrombin aptamers which form a cooperative complex only in the presence of target molecules, moving a methylene blue (MB)-conjugated oligonucleotide close to a gold electrode. Without washing steps, electrical current is increased in proportion to the concentration of a specific target protein. By employing a DNA-based experimental model with the aptamer system, we show that addition of a short DNA competitor can reduce background current of the MB peak to baseline levels. As such, the detection limit of aptamer-based ECPA for human thrombin was 50 pM via direct readout. The dual-probe nature of ECPA gave high selectivity and 93% recovery of signal from 2.5 nM thrombin in 2% bovine serum albumin (BSA). To greatly improve the flexibility of ECPA, we then proved the system functional with antibody-oligonucleotide conjugates as probes; the insulin detection limit was 128 fM with a dynamic range of over 4 orders of magnitude in concentration, again with high assay selectivity. ECPA thus allows separation-free, highly sensitive, and highly selective protein detection with a direct electrochemical readout. This method is extremely flexible, capable of detecting a wide variety of protein targets, and is amenable to point-of-care protein measurement, since any target with two aptamers or antibodies could be assayed via direct electrochemical readout.

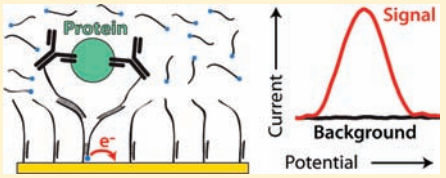

INTRODUCTION

Diagnostics is one of the most critical steps in health care and medical treatment.[1] Specific protein detection is of great importance in this realm, since it is currently one of the predominant methods to diagnose the onset or progression of disease states.[2,3] Unless specialized point-of-care assays are available for the protein of interest, quantitation is typically performed in a centralized laboratory by technicians.[4] This process is expensive and could waste time that is critical to patient care. Over the years, clinical approaches for point-of-care testing have addressed this challenge for select analytes,[5−9] yet these assay formats are highly specialized to the particular target molecule, thus inflexible to apply to other targets. To keep pace with expectations in future point-of-care testing, there is a need for more flexible, yet highly sensitive, quantitative, and easy-to-use methods.[4]

Although point-of-care devices are welcome in clinical and research laboratories, the existence of surrounding infrastructure places fewer constraints on methodology. Based on their inherent flexibility, sandwich enzyme-linked immunosorbent assays (ELISA) have emerged as the method of choice for protein quantitation in clinical and research laboratories.[3] Unfortunately, these heterogeneous assays require expert users with dedicated instrumentation, and they are time-consuming, laborious, and expensive. Quantitative, point-of-care protein analysis is thus not possible with standard sandwich ELISA formats. Nonetheless, the flexibility of the dual-antibody recognition concept is highly valuable and has served as a guide to various alternative strategies in recent years.[10−16]

Proximity immunoassays such as the proximity ligation assay (PLA)[11,12] or the molecular pincer assay[13] can overcome some of the limitations of ELISA. PLA, for example, is one of the most simple-to-use and sensitive protein assays developed to date.[17] The assay is homogeneous (no washing steps), and detection limits rival or outperform ELISAs, even with much smaller sample volumes. A key concept in PLA is the "proximity effect," which relies on simultaneous recognition of a target molecule by a pair of affinity probes. The bound probes can then be covalently linked by enzymatic ligation of their oligonucleotide tails, and qPCR is used as the readout, with products proportional to target protein concentration. PLA has been shown functional with aptamer pairs[11] and with a variety of antibody pairs.[12] Although nucleic acid aptamers have garnered significant attention in the analytical and biosensing communities based on their many potential advantages,[18−24] the use of aptamers as affinity probes in PLA is severely limited. PLA requires two aptamers binding at separate sites on the same protein target, but aptamer pairs unfortunately do not yet exist against most targets. In PLA[12] or in the pincer assays,[13] this limitation was overcome by employing antibody-oligonucleotide conjugates as probes, since the popularity and success of sandwich methodology (ELISA, Western blots) has afforded a large, commercially available library of antibody pairs against many proteins. These assays thus provide simpler and less expensive alternatives to ELISA.

Nonetheless, limitations in current proximity assays impede their use in a point-of-care setting. Although the use of qPCR gives PLA its high sensitivity, this readout requires that each sample be added to a tube with ligation and PCR reagents, and

Received: January 3, 2012
Published: March 27, 2012

dx.doi.org/10.1021/ja3000485 | J. Am. Chem. Soc. 2012, 134, 7066−7072

Table 1. Single-Stranded DNA Sequences Used in the ECPA Model Systems (Strategies 1 and 2)[a]

name	(abbreviation)	DNA sequence, listed 5′ to 3′
ECPA-loop	(loop)	TAG GAA AAG GAG GAG GGT GGC CCA CTT AAA CCT CAA TCC ACC CAC TTA AAC CTC AAT CCA CGC GGA TTT GAA CCC TAA CG
ECPA-MB-10	(MB-DNA)	CCA CCC TCC TCC TTT TCC TAT CTC TCC CTC GTC ACC ATG C/MB-C7/
ECPA-gold-10	(G10)	/5ThioMC6-D/GCA TGG TGA CAT TTT TCG TTC GTT AGG GTT CAA ATC CGC G
ECPA-gold-7	(G7)	/5ThioMC6-D/GCA TGG TAT TTT TCG TTC GTT AGG GTT CAA ATC CGC G
ECPA-gold-5	(G5)	/5ThioMC6-D/GCA TGA ATT TTC GTT CGT TAG GGT TCA AAT CCG CG
ECPA-Comp-9	(C9)	TCA CCA TGC
ECPA-Comp-8	(C8)	CAC CAT GC
ECPA-Comp-7	(C7)	ACC ATG C

[a]MB-DNA, G10, and C9 were employed in the optimized detection system. Abbreviations: /MB-C7/ = methylene blue modification (Biosearch), /5ThioMC6-D/ = disulfide bond flanked by two six-carbon spacers (IDT).

then be inserted into a qPCR instrument followed by 1−2 h of amplification and analysis. The molecular pincer assays are simpler and more rapid (<20 min), making them more amenable to point-of-care measurements by fluorescence readout; however, the limit of detection of these assays is several orders of magnitude higher than PLA. Thus, there is a need for a more sensitive yet simpler readout for proximity assays that is amenable to point-of-care testing.

Electrochemical detection is of particular interest in the development of biosensors because it offers great signal stability, simple instrumentation, high sensitivity, and ease of calibration compared to fluorescence, as well as excellent compatibility with miniaturization technologies.[25,26] Here, we present the marriage of the proximity assay concept with electrochemical detection to give a simple, highly sensitive, flexible strategy for specific protein quantitation, termed the electrochemical proximity assay (ECPA). ECPA uses the proximity effect to move an electrochemically active label, methylene blue (MB),[27] closer to a gold electrode upon binding of two probes to a protein target, an approach akin to electrochemical DNA sensing[28,29] or specialized aptamer-based protein sensing[30−32] reported by others. In the presence of protein targets, the redox current in ECPA is quantified using square wave voltammetry (SWV) and is found to depend directly on the concentration of target. This detection strategy is based largely upon pioneering work by the Plaxco group,[33−37] in using MB-labeled DNA for biosensing. Building upon this work and on aptamer-based protein sensing by Zhang et al.,[32] we have added the antibody-based proximity assay concept. We used a DNA-based experimental model to optimize signal-to-background ratios, ultimately providing a direct insulin detection limit that is lower than most commercially available ELISAs, with a dynamic range >40-fold wider than these ELISAs. These results were achieved with direct electrochemical readout, i.e., without requiring washing steps, which bodes well for the future of ECPA in point-of-care settings. In contrast to other approaches for electrochemical protein sensing,[24,30] ECPA should be useful for any protein with available antibody pairs.

EXPERIMENTAL DESIGN

Reagents and Materials. All solutions were prepared with deionized, ultrafiltered water (Fisher Scientific). The following reagents were used as received: insulin antibodies (clones 3A6 and 8E2; Fitzgerald Industries), 4-(2-hydroxyethyl)-1-piperazineethanesulfonic acid (HEPES) (99.5%), tris-(2-carboxyethyl) phosphine hydrochloride (TCEP), (Sigma-Aldrich, St. Louis, MO), bovine serum albumin (BSA, 98%; EMD Chemicals Inc.), human thrombin, immunoglobulin E (IgE), and insulin (Sigma Aldrich). Methylene blue-conjugated DNA (MB-DNA) was purchased from Biosearch Technologies (Novato, CA), purified by RP-HPLC. Oligonucleotides were obtained from Integrated DNA Technologies (IDT; Coralville, Iowa), with purity and yield confirmed by mass spectrometry and HPLC, respectively. Sequences (listed 5′ to 3′) for aptamer based ECPA were as follows. Thrombin aptamer A (THRaptA): AGTCCGTGGTAGGGCAGGTTGGGGTGACTTTTTTTTTTTTTTTTTTATATTTTTTTTTTCTCGCGGATTTGAACCCTAACG; Thrombin aptamer B (THRaptB): TAGGAAAAGGAGGAGGGTGGGATTGGTGTGTGTTTTTTTTTTTTTTTTTTTTTTTTTTTTTTGGTTGGTGTGGTTGG. Sequences (listed 5′ to 3′) for antibody-based ECPA were as follows. Insulin antibody arm 1 (AbArm1): /5AmMC6//iSp18/CCCACTTAAACCTCAATCCACGCGGATTTGAACCCTAACG; Insulin antibody arm 2 (AbArm2): TAGGAAAAGGAGGAGGGTGGCCCACTTAAACCTCAATCCA/iSp18//3AmMC6/. Sequences of ssDNA strands used in the experimental model are given in Table 1.

Preparation of the Electrode and DNA Monolayer Assembly. ECPA sensors for the model system, for thrombin detection, and for insulin detection were fabricated using a gold working electrode (Bioanalytical Systems Inc., r = 0.75 mm). The gold electrode was polished carefully to a mirror surface with an aqueous slurry of 0.05 μm diameter alumina particles and then successively washed in an ultrasonic cleaner with water. The electrode was then immersed into fresh piranha solution (H_2SO_4/H_2O_2, 3:1) for 5 min, rinsed with D. I. water, and dried under a stream of nitrogen gas. (Caution: piranha solution is dangerous to human health and should be used with extreme caution and handled only in small quantities). Finally, the gold electrode was electrochemically polished by scanning the potential from −0.5 to +1.5 V in 0.1 M H_2SO_4 at a scan rate of 0.1 V s^{-1} for 50 cycles. The cleaned gold electrode was thoroughly washed with D. I. water and ethanol and dried under flowing nitrogen.

Prior to modification of the electrode, 1 μL of 200 μM thiolated-DNA and 1 μL of 200 μM MB-DNA were each separately mixed with 2 μL of 10 mM TCEP in two 200-μL PCR tubes. These tubes were incubated for 90 min at room temperature (21 °C) for reduction of disulfide bonds in the thiolated-DNA and to reduce the MB-moiety of the MB-DNA. Both of these solutions were then diluted to a total volume of 200 μL in HEPES/$NaClO_4$ buffer (10 mM HEPES and 0.5 M $NaClO_4$, pH 7.0)[29] to a final concentration of 1 μM. Unless otherwise noted, all solutions used in the experiments to follow were carried out at pH 7.0. For immobilization, the previously cleaned gold electrode was transferred directly to the diluted and reduced thiolated-DNA solution and incubated for 16 h at room temperature in the dark. Following the formation of a self-assembled monolayer (SAM), excess thiolated-DNA physically adsorbed on the electrode surface was removed via a room temperature-deionized water rinse (~ 20 s). For all assay strategies employing the competitor DNA strands (most formats listed below), this same process was followed, except after reduction by 10 mM TCEP, the reduced thiolated-DNA solution was diluted to a total volume of 200 μL in HEPES/$NaClO_4$ buffer and incubated with 2 μM competitor DNA sequence (C9) for 60 min at room temperature in the dark. For immobilization in competitor systems, the cleaned gold electrode was transferred directly to this equilibrated thiolated-DNA/competitor solution then incubated for 16 h at room temperature in the dark.

dx.doi.org/10.1021/ja3000485 | J. Am. Chem. Soc. 2012, 134, 7066−7072

ECPA Probe Assembly and Electrochemical Measurements. Electrochemical measurements were performed using an Epsilon electrochemistry workstation (Bioanalytical Systems, Inc.) with a standard three-electrode configuration consisting of a Ag|AgCl(s)|KCl(sat) reference electrode (Bioanalytical Systems, Inc.), a home-made platinum gauze flag (0.77 cm^2) counter electrode, and a gold working electrode. All potentials are reported relative to the saturated Ag|AgCl reference electrode. Electrochemical measurements were performed in HEPES/$NaClO_4$ buffer using square wave voltammetry (SWV) with a 50 mV amplitude signal at a frequency of 60 Hz, over the range from −0.45 to 0.00 V versus Ag|AgCl reference. The characteristic voltammetric peak of MB was detected by SWV at −210 mV (vs Ag/AgCl). MB was chosen as the redox tag due to its excellent shelf life and robust electrochemical response in serum compared to other redox tags, such as ferrocene.[29,31] The electrochemical response of each sensor was measured as follows: (1) reference and measurement SWV data sets were collected; (2) both raw data sets were smoothed using a 21-point boxcar function and baseline corrected (all data corrected with B-spline generated baseline in Origin 8 using two regions: −0.40 to −0.35 V and −0.08 to 0.00 V); and (3) difference traces were generated. Signal (with target) and background (no target) voltammograms were treated in this manner and are presented as difference traces. To prepare calibration graphs and calculate standard deviations, traces were integrated from −0.330 to −0.100 V. In the case of the aptamer-based system, we report the average of three measurements, while in the case of the antibody-based system the average of two measurements is reported.

Model System Strategy 1: Decreasing Binding Affinity by Reducing the Number of Complementary Bases. The electrode was modified as described above and was placed into a glass electrochemical cell with HEPES/$NaClO_4$ buffer. Three different thiolated DNA sequences, G5, G7, and G10 (Table 1), were used in strategy 1 of the model system. In this way, the affinity of thiolated DNA and MB-DNA were adjusted through changes in the number of complementary bases between them. For modeling signal, the sensor was immersed in 10 nM ECPA-loop and 15 nM MB conjugated DNA sequences in 3 mL of HEPES/$NaClO_4$ buffer. For modeling background, the sensor was immersed in 15 nM MB conjugated DNA in 3 mL of HEPES/$NaClO_4$ buffer. Both signal and background currents were measured at the 15-min time point.

Model System Strategy 2: Use of a Short DNA Competitor. The electrode was modified as described above and was placed into a glass electrochemical cell with HEPES/$NaClO_4$ buffer. Three different competitor DNA sequences, C7, C8, and C9, were used in strategy 2 of the model system (Table 1). The sensor was allowed to equilibrate in 3 mL HEPES/$NaClO_4$ buffer with various concentrations of competitors for 6 h. For modeling background in the competitor systems, redox current was measured at each 10 min of the first hour, then at 90 and 120 min. Once C9 was chosen, 1:3, 1:7, 1:10, and 1:25 molar ratios of MB-DNA:C9 were tested at a fixed concentration of 15 nM MB-DNA.

Aptamer-Based ECPA System. The sensor was allowed to equilibrate in 3 mL of HEPES/$NaClO_4$ buffer with 100 nM C9 for 6 h. Thrombin aptamers (THRaptA and THRaptB) were first folded by heating to 95 °C and cooled rapidly by immersion in ice water to promote intramolecular interactions. Thrombin of various concentrations (from 50 pM to 50 nM) was incubated with folded 10 nM THRaptA and 15 nM THRaptB in HEPES buffer for 90 min prior to measurements. The thrombin/aptamer incubations were then added into the glass electrochemical cell. Before conducting voltammetric measurements, the sensor surface was allowed to react with analytes for 90 min. Selectivity tests with other proteins (IgE, insulin, or BSA) were made under the same conditions.

Antibody-Based ECPA System. The sensor was equilibrated in 500 μL of HEPES/$NaClO_4$ buffer with 300 nM C9 for 6 h. Prior to measurements, HEPES/$NaClO_4$ buffer was supplemented with 0.5% BSA (w/v) (to minimize antibody adsorption), 10 nM Ab1, 10 nM Ab2, and 10 nM MB (for background measurements), and various concentrations of insulin (from 128 fM to 2 nM). Before conducting voltammetric measurements, the sensor surface was allowed to react with analytes for 40 min. Selectivity tests were performed in the same manner by substituting 2 nM C-peptide or insulin-like growth factor 1 (IGF-1) for insulin.

Preparation of Antibody-Oligonucleotide Conjugates. The antibody-oligonucleotide conjugates used in the insulin ECPA, AbArm1-3A6 and AbArm2-8E2, were prepared by conjugating AbArm1 to insulin antibody 3A6 ($K_d \approx 1$ nM) and AbArm2 to insulin antibody 8E2 ($K_d \approx 0.1$ nM), respectively (antibodies obtained from Fitzgerald Industries). Conjugation reactions and purification steps were accomplished using an Antibody-Oligonucleotide All-In-One Conjugation Kit (Solulink), according to the manufacturer's instructions. Briefly, the oligonucleotides were first activated with sulfo-S-4FB, and their quantities and qualities were confirmed using absorbance, specifically $A_{260\ nm}$ of unmodified activated oligonucleotides and the $A_{260\ nm}$ to $A_{360\ nm}$ ratio after the modification of activated oligonucleotides. Antibodies were also activated with S-HyNic. Activated oligonucleotides and antibodies were then mixed and incubated at room temperature for 2 h. Once the conjugation reaction was stopped, conjugates were further purified using the supplied magnetic affinity matrix. The final concentrations of the conjugates were determined by the Bradford protein assay. AbArm1-3A6 and AbArm2-8E2 were synthesized with 45% and 86% recovery from the initial amount of antibodies (100 μg).

RESULTS AND DISCUSSION

Signal and Background in ECPA. The principle of the electrochemical proximity assay (ECPA) is shown in Figure 1.

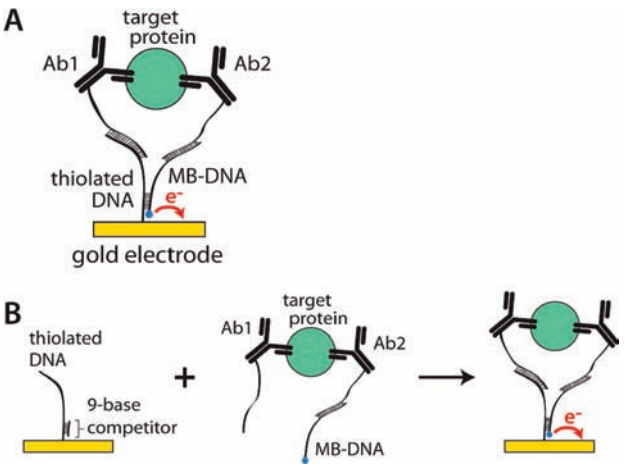

Figure 1. Principle of the electrochemical proximity assay (ECPA). In the presence of the target protein, this five-part complex moves the redox-active methylene blue (MB) near the gold surface, thus increasing current in proportion to the protein analyte. Depicted here are (A) the final, five-part cooperative complex and (B) the stepwise operation of the assay, in which the electrode with a preassembled DNA/competitor monolayer is immersed into a premixed solution of EPCA probes (two Ab-oligos and MB-DNA) and target protein to generate current.

The sensor is prepared by self-assembly of thiolated DNA strands onto a gold electrode via the alkanethiol moiety at the 5′ terminus. The quantitative capacity of ECPA stems from cooperative hybridization of the five-part complex shown in Figure 1: thiolated DNA−DNA conjugated antibody 1−target protein−DNA conjugated antibody 2−MB conjugated DNA. The five-part complex forms a circular structure on the sensor surface through proximity-dependent hybridization of the thiolated DNA and MB-DNA, which is the step that brings MB close enough to the gold electrode surface for electrochemical

dx.doi.org/10.1021/ja3000485 | J. Am. Chem. Soc. 2012, 134, 7066−7072

current enhancement. This process results in a quantity of electrons transferred from MB to the electrode that is proportional to the original amount of protein analyte ("signal"), albeit with some analyte-independent current generated by hybridization of thiolated DNA and MB-DNA only ("background"). Although SWV does not differentiate signal and background currents, under optimized conditions, the signal will greatly exceed the background to allow highly sensitive, direct electrochemical quantitation of the protein analyte. Similar to what has been observed in PLA[11,17] or the molecular pincer assays,[13] signal enhancement over background in ECPA is based on the proximity effect, that is, the marked increase in the effective concentrations of the MB-DNA and thiolated DNA due to the simultaneous binding of the two probes to the same protein. This allows the MB-DNA/thiolated DNA interaction to be weak in the absence of protein ("background") yet strong in the presence of the protein ("signal"). Finally, it should be noted that the detection limits of proximity assays are often well below the K_d values of the individual probes, which can be attributed to the chelate-like effect of utilizing two probes in a cooperative fashion, often termed the "proximity effect."

Through binding equilibria, a fraction of thiolated DNA will always hybridize with the MB-DNA sequences, even in the absence of target analyte, resulting in target-independent hybridization, recruitment of MB to the gold surface, and an increase in current. A portion of this background current could also result from nonspecific adsorption of MB-DNA to the surface, although our results suggest that specific binding is the major cause. The presence of this background current is obviously detrimental to the assay. We applied two strategies in attempt to lower the background using our model system, as discussed below.

DNA-Based Experimental Model of ECPA. As in our previous work with PLA,[17] here we utilized a DNA loop to model the probe-target complex in ECPA (Figure 2A), making the assumption that probe affinity for the target protein is infinite. The 80-nucleotide DNA loop mimics formation of the ECPA complex, bringing MB near the gold surface and increasing redox current. The background was modeled using only the thiolated DNA and MB-DNA (Figure 2A). This experimental model greatly simplified the optimization of experimental parameters. Since the surface-dependent ECPA involves a different type of cooperative complex formation compared to homogeneous PLA, we devised two new strategies for minimizing background in ECPA.

The first strategy was to decrease the binding affinity between thiolated DNA and MB-DNA by reducing the number of complementary bases in the thiolated DNA (Figure 2B). The hypothesis was that the amount of background hybridization between thiolated DNA and MB-DNA would be greatly reduced, thereby reducing background current greatly without a large decrease in signal current. Figure 2C compares the signal and background responses of the system with 5, 7, and 10 complementary bases (G5, G7, and G10 strands). Comparing G10 to G7, as hypothesized, the background current was reduced by 2-fold while signal current was reduced by only 1.6-fold. Furthermore, compared to a background peak current of 54 nA with G10, it was indeed possible to reduce the background current to baseline using G5. However, the background reduction was accompanied by a large decrease in signal peak current from 104 nA down to 38 nA, since the weakened connection also weakened hybridization of the DNA Loop (model of signal).

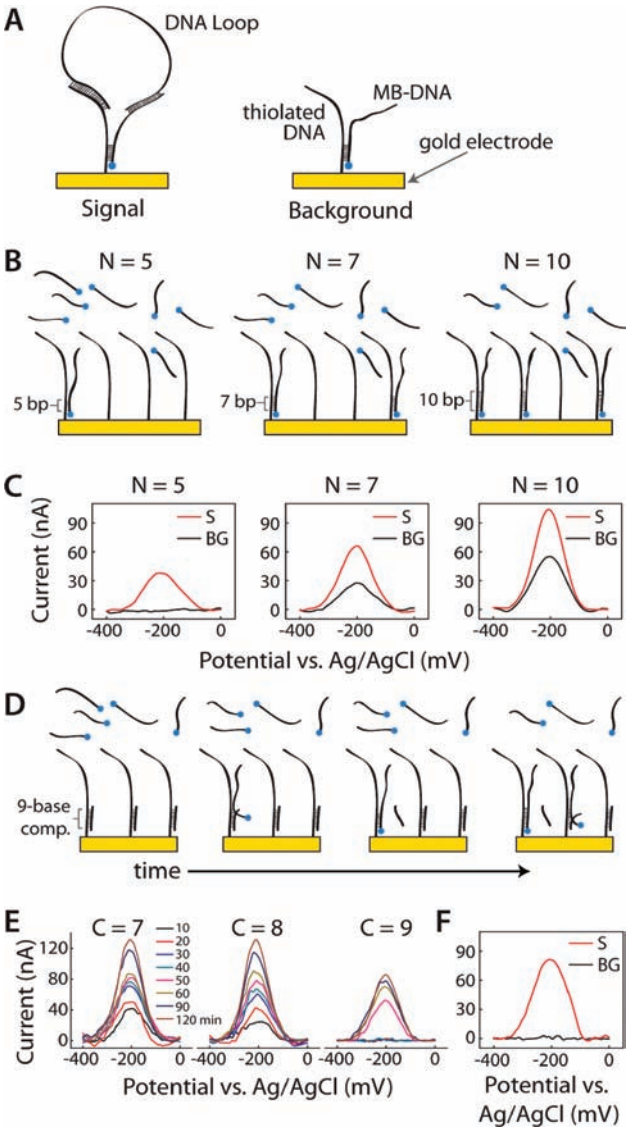

Figure 2. DNA-based model for ECPA. (A) A continuous DNA loop is used to model the Signal complex shown in Figure 1. Background is modeled by simply adding MB-DNA without the loop. (B) Depiction of background reduction in strategy 1. Fewer base pairs (weaker hybridization) between thiolated DNA and MB-DNA results in lower background current. (C) Experimental confirmation of strategy 1, with both signal and background currents reduced in the voltammograms as the number of base pairs (N) is reduced. At $N = 5$, background is minimized, but signal is reduced significantly. (D) Depiction of background reduction in strategy 2, where a competitor strand prevents or slows background formation over a given time window. (E) Experimental confirmation of strategy 2. The 9-base competitor (C9) was the only one to show baseline current for up to 40 min. (F) Signal and background voltammograms are shown with C9 under optimal conditions, showing more than double the signal current and equal background current compared to $N = 5$ from strategy 1.

In an attempt to reduce background without such a large signal reduction, our second strategy was to utilize a short DNA competitor with the G10 system. We hypothesized that when using a competitor sequence, background hybridization would occur more slowly than signal hybridization, since both signal and background complexes must displace the short competitor prior to current enhancement by the MB-DNA strand. Figure 2D shows a representation of the delayed background formation over

dx.doi.org/10.1021/ja3000485 | J. Am. Chem. Soc. 2012, 134, 7066−7072

time, mediated by competition with competitor strands. This way, signal of similar magnitude to that in the $N = 10$ case above should form rapidly, while background would be delayed kinetically by the competitor. Figure 2E shows signal and background responses of the system with 7-, 8-, and 9-base competitors (C7, C8, and C9). As hypothesized, the hybridized competitor sequences blocked access of MB-DNA to the thiolated DNA, thereby slowing background formation. Figure 2E shows that with C7 and C8, background currents of 47 and 24 nA were detected even 10 min after addition of MB-DNA, while no background was detected for as long as 40 min using C9. Since C9 allowed a 40-min time window for detection, we chose C9 as the competitor for further experiments. Upon addition of the Loop (model of signal), significant signal current of 81 nA was possible after 30 min, while C9 prevented background formation (Figure 2F). Optimal conditions were determined to be 15 nM MB-DNA and 100 nM C9, and these were applied in the aptamer-based ECPA system, below.

Aptamer-Based ECPA. A schematic of aptamer-based ECPA is shown in Figure 3A (upper right). Two thrombin aptamers (THRaptA, THRaptB) that bind thrombin at different sites were applied as affinity probes, and competitor C9 was used to minimize background. Using conditions optimized by the model system, background levels were measured in the absence of target protein (human thrombin). Similar to the model system, background remained at baseline current for up to 90 min, after which an increasing peak current at −210 mV was detected, indicating that MB-DNA was beginning to displace the competitors. This 90-min detection window was actually wider than the 40-min window observed in the model system. This difference is attributed to the decreased diffusion coefficient[38] of the MB-DNA (40-bases; ∼70 $\mu m^2\ s^{-1}$) when hybridized with THRaptB (120-bases; ∼30 $\mu m^2\ s^{-1}$), which would slow the kinetics of the competitor displacement process by ∼2.3-fold in comparison to the model system. This estimation agrees very well with the 2.25-fold increase in time required for background formation. The lower right plot in Figure 3A shows the background with no thrombin (black trace) and a typical MB oxidation peak appearing at −210 mV (red trace) in the presence of 2.5 nM thrombin after the 90 min incubation. As expected, the saturated peak current at 10 nM thrombin (52 nA) was of lower magnitude than the model system (81 nA), which had assumed probes with infinite affinity. This aptamer-based ECPA system calibrated versus thrombin concentration (Figure 3A, left plot), with sensor responses recorded in triplicate as integrated MB peak areas from −330 to −100 mV. ECPA was capable of detecting thrombin levels as low as 50 pM using a direct electrochemical readout, with a dynamic range up to 10 nM at these probe concentrations.

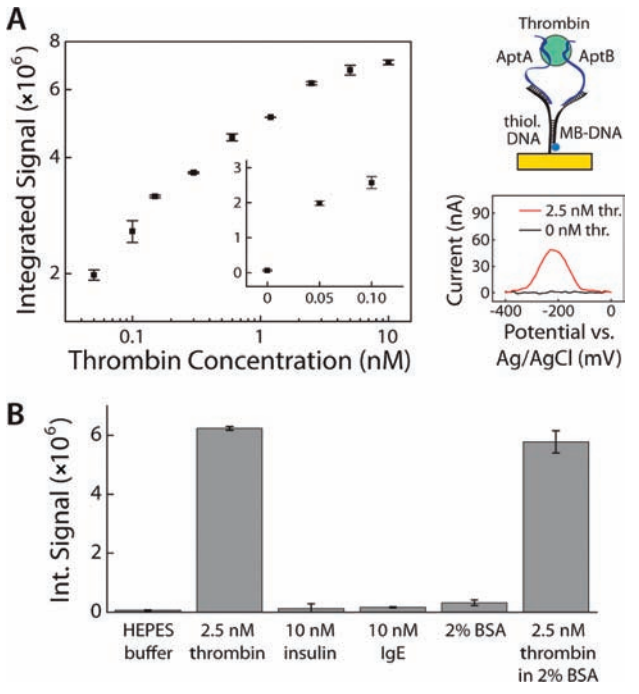

Figure 3. Aptamer-based ECPA. (A) With a direct readout, a human thrombin detection limit of 50 pM was achieved, with a dynamic range up to 10 nM. Upper right image shows the principle of the assay, with the lower right plot showing example voltammagrams for the blank (black) and in the presence of 2.5 nM thrombin (red). (B) The dual-probe assay shows high selectivity, as expected, with 93% recovery of signal in the presence of 2% BSA.

To demonstrate specificity, the aptamer-based ECPA was challenged with nonspecific proteins including human IgE, insulin, and BSA. Figure 3B shows that essentially no response was observed in the presence of 10 nM insulin or IgE; even with 4-fold lower thrombin (2.5 nM), the signal was ∼40-fold larger than that of IgE or insulin. In addition, baseline current was observed in the presence of 2% BSA, while the signal from 2.5 nM thrombin was recovered by 93% in 2% BSA. This result is encouraging for future application of ECPA to biological samples and point-of-care settings.

Antibody-Based ECPA. The flexibility of the aptamer-based approach is limited because of the requirement of two aptamers for the target protein, since aptamer pairs exist only for a few select proteins. As noted above, the use of antibody-oligonucleotide conjugates as probes can overcome this challenge.[12,13] With the success of sandwich immunoassays, there exists a large, commercially available library of antibody pairs against many proteins. As proof of concept that ECPA can be applied to a wide variety of protein targets, we show herein that insulin can be directly detected using two antibody-oligonucleotide conjugates as ECPA probes.

A schematic of antibody-based ECPA is shown in Figure 4A (upper right), again employing the short DNA competitor strategy. With this new assay format, a different set of conditions were determined as optimal, including the addition of 0.5% BSA to reduce nonspecific antibody adsorption and a C9 concentration of 300 nM. Using 10 nM of each antibody-oligo and 10 nM MB-DNA, the assay showed a 40-min detection window before competitor began to be displaced by MB-DNA. Since the antibody-oligo conjugates will significantly alter the diffusion rates of most components, we did not expect the kinetics of signal and background formation to follow trends observed in the model system or aptamer-based ECPA; nonetheless, the detection time window was similar to the other systems. The lower right plot in Figure 3A shows the background with no insulin (black trace) and a typical MB oxidation peak appearing at −210 mV (red trace) in the presence of 2 nM insulin after 40 min. This antibody-based ECPA system was then calibrated versus insulin concentration (Figure 4A, left plot), with sensor response recorded in duplicate as integrated MB peak areas from −330 to −100 mV. Remarkably, using a direct electrochemical readout, ECPA was capable of detecting insulin levels as low as 128 fM (7.43×10^{-4} ng mL^{-1}) with a dynamic range extending to 2 nM (11.6 ng mL^{-1}). The selectivity of

dx.doi.org/10.1021/ja3000485 | J. Am. Chem. Soc. 2012, 134, 7066−7072

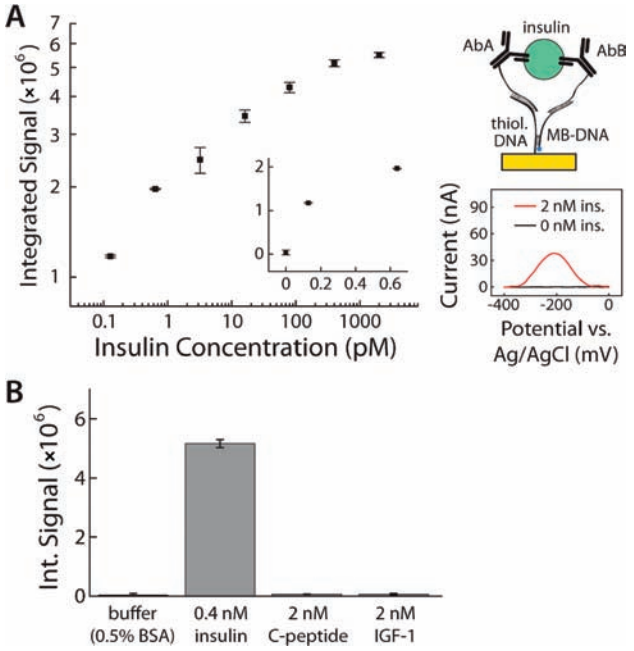

Figure 4. Success of antibody-based ECPA greatly improves the flexibility of the assay, since a large variety of protein targets could be quantified this way. (A) Insulin as low as 128 fM was detected with direct readout, with a dynamic range up to 2 nM. Upper right image shows the principle of the assay, with the lower right plot showing example voltammagrams for the blank (black) and in the presence of 2 nM insulin (red). (B) The dual-antibody assay also shows high selectivity, as expected.

antibody-based ECPA was tested against insulin-like growth factor 1 (IGF-1), which has similar structure to insulin, and against C-peptide, which is cosecreted with insulin into the bloodstream. As expected, the sensor did not respond to higher concentrations of either IGF-1 or C-peptide (Figure 4B). The drastically improved performance of the antibody-based ECPA compared to the thrombin aptamer ECPA was expected, since the aptamer K_d values[39] are several orders of magnitude higher than the typical antibody K_d.

Finally, Table 2 shows a comparison of our antibody-based ECPA to commercially available sandwich ELISAs for insulin detection.[40−45] In order to facilitate equal comparison of the direct-readout ECPA with various heterogeneous ELISAs, the concentrations of insulin in the incubation solution of each ELISA is reported in Table 2. ECPA outperforms all of the kits in terms of assay dynamic range (from 43- to 312-fold wider range). The impresssive ECPA dynamic range of 15 600 (from 128 fM to 2 nM) should provide enhanced flexibility in sample preparation. Only one of the "ultrasensitive" versions of ELISA (25-μL sample volume) has an essentially equal detection limit (1.1-fold higher) compared to ECPA. Compared to "standard" ELISA kits, ECPA shows between 15.6- and 60.9-fold lower limit of detection for insulin. In fact, using the noise level of the blank, the linearly extrapolated LOD for insulin was calculated to be 20 fM, lower than all ELISAs shown in Table 2. These performance improvements come with the additional benefit of a direct-readout format, making ECPA amenable to point-of-care analysis. To our knowledge, ECPA represents the highest performing direct-readout insulin assay reported to date. Looking toward future application in point-of-care insulin measurements in human serum, if we leverage the pioneering efforts of the Plaxco group using similar DNA-based electrochemical sensors,[28,29,33−37] it should be possible to detect a variety of proteins in undiluted serum. Of course, since the ECPA detection limit for insulin (128 fM) is over 400-fold lower than the normal human serum insulin levels (~60−80 pM), serum samples could be simply diluted to minimize interferences in this case.

■ CONCLUSIONS

In this paper, we describe the development of the electrochemical proximity assay (ECPA), which leverages two aptamer or antibody-oligonucleotide probes and proximity-dependent DNA hybridization to move a redox active molecule near a gold electrode. A DNA-based experimental model was used to optimize the assay format, and aptamer- and antibody-based ECPA were shown functional with high sensitivities and low detection limits, employing a short DNA competitor to limit background current. This background-reduced ECPA was shown to match or outperform currently used ELISA kits for insulin detection.

Of particular importance is the proof-of-concept provided by antibody-based ECPA. Judging from to the successes of other proximity immunoassays,[12,13] it is reasonable to assume that ECPA should perform well in quantifying any other protein with an available antibody pair. Combining the assay's flexibility and high sensitivity with the simplicity of direct electrochemical readout, ECPA should be useful in a variety of settings in the future, including medical diagnostics, biological research, and point-of-care testing.

Table 2. Performance Comparisons between ECPA and Various Commercially Available ELISA Kits[a]

assay	analyte	LOD (fM)	relative LOD (LOD_{ELISA}/LOD_{ECPA})	dynamic range	relative range ($range_{ECPA}/range_{ELISA}$)	citation
ECPA	human insulin	128	1	15 600	1	present work
ELISA[b]	human insulin standard	5200	41	100	160	40
		2000	16	200	80	41
		7800	61	75	210	42
	ultrasensitive	140	1.1	290	50	43
	mouse insulin standard	3100	24	50	310	44
	ultrasensitive	820	6.4	360	40	45

[a]ECPA has a lower detection limit than five of the six kits in the table (as much as 60-fold lower), with a comparable detection limit to one 'ultrasensitive' human insulin ELISA. The dynamic range of ECPA is >40-fold wider than all ELISAs shown in the table (as much as 300-fold wider). These improvements shown by ECPA come with the added benefit of a direct electrochemical readout, i.e., without requiring washing steps. Abbreviations: ECPA = electrochemical proximity assay, ELISA = enzyme-linked immunosorbent assay, LOD = limit of detection. [b]To provide valid method comparisons, LODs and dynamic ranges for ELISAs are defined by the concentrations in the incubation mixture, prior to the washing step and secondary antibody incubation.

dx.doi.org/10.1021/ja3000485 | J. Am. Chem. Soc. 2012, 134, 7066−7072

AUTHOR INFORMATION

Corresponding Author

shanncg@auburn.edu; chris.easley@auburn.edu

Author Contributions

†These authors contributed equally.

Notes

The authors declare no competing financial interest. The ECPA methodology presented in this article was included in a U.S. Provisional Patent Application (No. 61546842) filed by C.J.E., C.S., J.H., and T.W. on October 13, 2011.

ACKNOWLEDGMENTS

The authors would like to thank Prof. David Stanbury for use of instrumentation for square wave voltammetry. Funding for this work was provided by the National Science Foundation, CBET-1067779 (CJE); by the U.S. Department of Agriculture, 2009–34605–19805O (CS); and by the Department of Chemistry and Biochemistry at Auburn University.

REFERENCES

(1) Martinez, A.; Phillips, S. T.; Whitesides, G. M.; Carrilho, E. *Anal. Chem.* **2010**, *82*, 3–10.

(2) Burtis, C. A.; Ashwood, E. R. *Tietz Textbook of Clinical Chemistry*; Saunders: Philadelphia, PA, 1999.

(3) Rusling, J. F.; Kumar, C. V.; Gutkind, J. S.; Patel, V. *Analyst* **2010**, *135*, 2496–2511.

(4) von Lode, P. *Clin. Biochem.* **2005**, *38*, 591–606.

(5) Sorell Gómez, L.; Rojas, G. *Clin. Chim. Acta* **1997**, *260*, 65–71.

(6) Jung, K.; Zachow, J.; Lein, M.; Brux, B.; Sinha, P.; Lenk, S.; Schnorr, D.; Loening, S. A. *Urology* **1999**, *53*, 155–160.

(7) Stivers, C. R.; Baddam, S. R.; Clark, A. L.; Ammirati, E. B.; Irvin, B. R.; Blatt, J. M. *Diabetes Technol. Ther.* **2000**, *2*, 517–526.

(8) Davies, S; Byrn, F; Cole, L. A. *Clin. Lab. Med.* **2003**, *23*, 257–264.

(9) Seamark, D. A.; Backhouse, S. N.; Powell, R. *Ann. Clin. Biochem.* **2003**, *40*, 178–180.

(10) Haab, B. B.; Dunham, M. J.; Brown, P. O. *Genome Biol.* **2001**, *2*, 1–S.

(11) Fredriksson, S.; Gullberg, M.; Jarvius, J.; Olsson, C.; Pietras, K.; Gustafsdottir, S. M.; Ostman, A.; Landegren, U. *Nat. Biotechnol.* **2002**, *20*, 473–477.

(12) Gullberg, M.; Gustafsdottir, S. M.; Schallmeiner, E.; Jarvius, J.; Bjarnegård, M.; Betsholtz, C.; Landegren, U.; Fredriksson, S. *Proc. Natl. Acad. Sci. U.S.A.* **2004**, *101*, 8420–8424.

(13) Heyduk, E.; Dummit, B.; Chang, Y. H.; Heyduk, T. *Anal. Chem.* **2008**, *80*, 5152–5159.

(14) Konry, T.; Hayman, R. B.; Walt, D. R. *Anal. Chem.* **2009**, *81*, 5777–5782.

(15) Kim, D.; Daniel, W. L.; Mirkin, C. A. *Anal. Chem.* **2009**, *81*, 9183–9187.

(16) Luminex Corporation, Technologies and Science, http://www.luminexcorp.com/TechnologiesScience/index.htm; accessed December 2011.

(17) Kim, J.; Hu, J.; Sollie, R. S.; Easley, C. J. *Anal. Chem.* **2010**, *82*, 6976–6982.

(18) Osborne, S. E.; Ellington, A. D. *Chem. Rev.* **1997**, *97*, 349–370.

(19) Famulok, M. *Curr. Opin. Struct. Biol.* **1999**, *9*, 324–329.

(20) Drummond, T. G.; Hill, M. G.; Barton, J. K. *Nat. Biotechnol.* **2003**, *21*, 1192–1199.

(21) *The Aptamer Handbook. Functional Oligonucleotides and Their Applications*; Klussmann, S., Ed.; WILEY-VCH Verlag GmbH & Co. KGaA: Weinheim, Germany, 2006.

(22) Herr, J. K.; Smith, J. E.; Medley, C. D.; Shangguan, D.; Tan, W. *Anal. Chem.* **2006**, *78*, 2918–2924.

(23) Shangguan, D.; Li, Y.; Tang, Z.; Cao, Z. C.; Chen, H. W.; Mallikaratchy, P.; Sefah, K.; Yang, C. J.; Tan, W. *Proc. Natl. Acad. Sci. U.S.A.* **2006**, *103*, 11838–11843.

(24) Liu, Y.; Tuleouva, N.; Ramanculov, E.; Revzin, A. *Anal. Chem.* **2010**, *82*, 8131–8136.

(25) Hianik, T.; Wang, J. *Electroanalysis* **2009**, *21*, 1223–1235.

(26) Sassolas, A.; Blum, L. J.; Leca-Bouvier, B. D. *Electroanalysis* **2009**, *21*, 1237–1250.

(27) Kelley, S. O.; Barton, J. K.; Jackson, N. M.; Hill, M. G. *Bioconjug. Chem.* **1997**, *8*, 31–37.

(28) Fan, C.; Plaxco, K. W.; Heeger, A. J. *Proc. Natl. Acad. Sci. U.S.A.* **2003**, *100*, 9134–9137.

(29) Kang, D.; Zuo, X.; Yang, R.; Xia, F.; Plaxco, K. W.; White, R. J. *Anal. Chem.* **2009**, *81*, 9109–9113.

(30) Zhang, Y. L.; Huang, Y.; Jiang, J. H.; Shen, G. L.; Yu, R. Q. *J. Am. Chem. Soc.* **2007**, *129*, 15448–15449.

(31) Ferapontova, E. E.; Olsen, E. M.; Gothelf, K. V. *J. Am. Chem. Soc.* **2008**, *130*, 4256–4258.

(32) Zhang, Y. L.; Pang, P. F.; Jiang, J. H.; Shen, G. L.; Yu, R. Q. *Electroanalysis* **2009**, *21*, 1327–1333.

(33) Bonham, A. J.; Hsieh, K.; Ferguson, B. S.; Vallée-Bélisle, A.; Ricci, F.; Soh, H. T.; Plaxco, K. W. *J. Am. Chem. Soc.* **2012**, *134*, 3346–3348.

(34) Vallée-Bélisle, A.; Ricci, F.; Plaxco, K. W. *J. Am. Chem. Soc.* **2012**, *134*, 2876–2879.

(35) Xia, F.; Zuo, X.; Yang, R.; White, R. J.; Xiao, Y.; Kang, D.; Gong, X.; Lubin, A. A.; Vallée-Bélisle, A.; Yuen, J. D.; Hsu, B. Y.; Plaxco, K. W. *J. Am. Chem. Soc.* **2010**, *132*, 8557–8559.

(36) Rowe, A. A.; Chuh, K. N.; Lubin, A. A.; Miller, E. A.; Cook, B.; Hollis, D.; Plaxco, K. W. *Anal. Chem.* **2011**, *83*, 9462–9466.

(37) Lubin, A. A.; Plaxco, K. W. *Acc. Chem. Res.* **2010**, *43*, 496–505.

(38) Nkodo, A. E.; Garnier, J. M.; Tinland, B.; Ren, H.; Desruisseaux, C.; McCormick, L. C.; Drouin, G.; Slater, G. W. *Electrophoresis* **2001**, *22*, 2424–2432.

(39) Hu, J.; Easley, C. J. *Analyst* **2011**, *136*, 3461–3468.

(40) Millipore Corportation, Human Insulin ELISA, http://www.millipore.com/catalogue/item/ezhi-14k; accessed December 2011.

(41) Mercodia AB, Insulin ELISA, http://www.mercodia.se/index.php?page=productview2&prodId=9; accessed December 2011.

(42) AbCam plc., Insulin Human ELISA Kit – 1 × 96 Well Plate (ab100578), http://www.abcam.com/Insulin-Human-ELISA-Kit-1-x-96-Well-Plate-ab100578.html; accessed December 2011.

(43) Mercodia AB, Insulin, Ultrasensitive ELISA, http://www.mercodia.se/index.php?page=productview2&prodId=11; accessed December 2011.

(44) Millipore Corporation, Rat/Mouse Insulin ELISA, http://www.millipore.com/catalogue/item/ezrmi-13k; accessed December 2011.

(45) ALPCO Diagnostics, Mouse Ultrasensitive Insulin ELISA, 80-INSMSU-E01, http://www.alpco.com/products/Insulin_Ultrasensitive_Mouse_ELISA.aspx; accessed December 2011.